4ème Conférence Internationale des Energies Renouvelables (CIER-2016)
Proceedings of Engineering and Technology – PET
Vol.16, pp.78 - 84

Conventional and Adaptive Sliding Mode for Active and Reactive Power Control of Doubly Fed Induction Generator Wind Turbines

Mbarek TALEB*, Mohamed CHERKAOUI

EMI (Ecole Mohammadia d'Ingénieurs), Mohammed V University, Department of Electrical Engineering, Rabat, Morocco

***Abstract*—In this paper, a novel adaptive sliding mode controller (ASMC) is used to control active and reactive power of a Wind Energy Conversion System(WECS) equipped with Doubly Fed Induction Generator (DFIG). The control is based on a P-Q decoupled strategy that allows easy adaptation to the new grid codes. The performances of this controller are compared with Conventional Sliding Mode Controllers (SMC) through simulation on MATLAB/Simulink software to show its efficiency.**

***Index Terms*—DFIG, variable speed wind turbine, power control, PI control, SMC, ASMC.**

I. INTRODUCTION

Renewable energy sources such as solar, wind, geothermal, sea energy (tidal and wave) emerged as a solution for global warming effect, population growth, fossil-fuel depletion and its insecure transportation

Among all these alternative renewable sources, wind energy received a great interest and become the fastest growing energy by rising from 59GW on 2005 to 433GW on 2015 [1]. It is expected to reach 759GW by 2020 and 1600GW by 2030 supplying more than 20% of worldwide power [2, 3].

The success of this energy is in part due to the fact that its cost has gone down by more than 80% since the early 1980's [4]. Now, in many countries we can find offers at less than 4 cents per KWH even less than 3 cents in USA [4] and in Morocco [5].

However, integration into the electrical network of a large scale wind power is impacting the grid's power quality. That is why transmission system operators (TSOs) in many countries are issuing grid code to regulate the connection of wind power installations to the grids.

In wind energy conversion systems, many topologies are used [6], but the most popular is which uses DFIG for which stator is connected directly to the grid while the rotor is connected to grid through a double bi-directional converters separated by a DC-Link [7] as shown in fig.1.

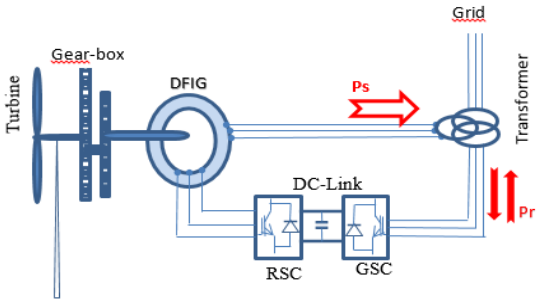

Fig. 1. Synoptic scheme of DFIG Wind Energy Conversion System

A lot of approaches are used to control DFIG WECS for different purposes, but most of them deal with speed or torque control for MPPT purpose and with reactive power to assure unit power factor in vast majority of cases. Few works have been dealing with PQ control to answer any powers profiles desired by Grid Managers.

Linear algorithms such as PI, in spite of their simplicity as well as their performances in permanent state, are little used in WECS because of their limitation to face parameters variations and to fight with strong intrinsic nonlinearities.

Nonlinear algorithms based on Artificial Intelligence (AI) have received a great interest since last decade because they are suitable for processes that have strong intrinsic nonlinearities and parameters variations. Among these, the most popular are Fuzzy Logic Controller (FLC) [8, 9], Neuronal Network Controller (NNC) [10] and Particle Swarm Optimization (PSO) [11]. These algorithms are generally relatively complex and need trial and error to settle their parameters. They are still not mature for WECS domain. In literature concerning WECS, these algorithms applied to control power flow give in general good tracking reference but unsatisfactory exceeding rates (between 10 and 20%).

In contrast, classical nonlinear algorithms such as SMC and its derivative ASMC are more familiar and widely used in varied fields. They are easier and more appropriate for WECS and generally give better performances. Consequently, we opted for basic SMC that gives satisfactory results (6% only of exceeding rate for active

ISSN 2356-5608

power and 11% for reactive power) along with good robustness to parameters variations. Then, these results are drastically improved by modifying the SMC to an ASMC by making its gain variable according to a new algorithm. This latter was used first time by [12] to control a pneumatic actuator. We have slightly adapted it to our case. All dynamics performances are really irreproachable.

This paper is organized as follow: Next section (section II) gives the modelling of the wind turbine and presents MPPT strategy and how PQ approach is important for new grid codes, followed by section III where DFIG is modelled for power control purpose. section IV is divided to three subsections that present respectively SMC, ASMC and simulations results. Finally, conclusion is provided in last section.

II. MODELLING OF THE WIND TURBINE

A part of Kinetic energy of the wind is captured by turbine blades according to a power coefficient, specific to each turbine [13]:

$$C_p(\lambda,\beta) = C_1\left(\frac{C_2}{\lambda_i} - C_3\beta - C_4\right)\exp\left(-\frac{C_5}{\lambda_i}\right) + C_6\lambda$$
$$\frac{1}{\lambda_i} = \frac{1}{\lambda + 0.08\beta} - \frac{0.035}{1+\beta^2} \qquad (1)$$

β is the blade pich angle and $\lambda = \frac{R\omega_t}{v}$ is the tip speed ratio where R and ω_t are respectively rotor radius and rotor speed of the turbine and v the wind speed.

$C_p(\lambda,\beta)$ illustrated on Fig. 2 cannot exceed the Betz limit $16/27 \simeq 0.59$ and his optimal value in our case is $C_{p-opt} \simeq 0.48$ obtained for $\beta = 0$ and $\lambda = \lambda_{opt} \simeq 8$.

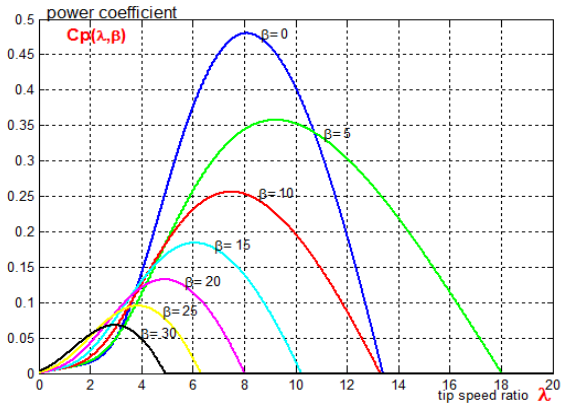

Fig. 2. Power Coefficient Variations against λ and β.

The popular approach called MPPT (Maximum Power Point Tracking) is widely used in WECS and it consists to adjust the Generator speed to capture the Maximum Power from the wind for any wind speed v as shown in Fig. 3.

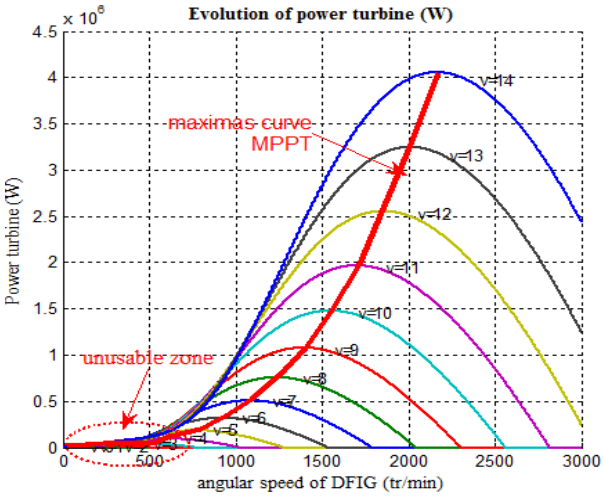

Fig. 3. Turbine Power Variations against Angular Speed of DFIG.

MPPT stays a particular case of the PQ approach as new grid codes are dictating now profiles for active and reactive powers.

As an example, German grid code asks wind farmes to reduce active power by 40% for each 1Hz of extra elevation of frequency (gradient $\frac{\Delta P}{\Delta f} = 0.4$) while reactive power must be able to vary from -30% (absorption) to +30% (production) [14].

III. MODELLING OF THE DFIG

DFIG is described in the d-q Park reference frame rotating at synchronous speed ω_s as follow [15]:

$$\begin{cases} v_{sd} = R_s i_{sd} + \frac{d\phi_{sd}}{dt} - \omega_s \phi_{sq} \\ v_{sq} = R_s i_{sq} + \frac{d\phi_{sq}}{dt} + \omega_s \phi_{sd} \\ v_{rd} = R_r i_{rd} + \frac{d\phi_{rd}}{dt} - \omega_r \phi_{rq} \\ v_{rq} = R_r i_{rq} + \frac{d\phi_{rq}}{dt} + \omega_r \phi_{rd} \end{cases} \qquad (2)$$

With:

$$\begin{cases} \phi_{sd} = L_s i_{sd} + M i_{rd} \\ \phi_{sq} = L_s i_{sq} + M i_{rq} \\ \phi_{rd} = L_r i_{rd} + M i_{sd} \\ \phi_{rq} = L_r i_{rq} + M i_{sq} \end{cases} \qquad (3)$$

The active and reactive powers at the stator side of DFIG are defined by

$$P_s = v_{sd} i_{sd} + v_{sq} i_{sq} \text{ and } Q_s = v_{sq} i_{sd} - v_{sd} i_{sq} \qquad (4)$$

ISSN 2356-5608

The electromagnetic torque is given by :

$$C_{em} = p(\phi_{sd} i_{sq} - \phi_{sq} i_{sd}) \quad (5)$$

To simplify equations, we opted for aligning the stator flux on the d-axis to obtain:

$$\phi_{sd} = \phi_s \text{ and } \phi_{sq} = 0 \quad (6)$$

Hence,

$$\begin{cases} v_{rd} = (R_r + p\sigma L_r) i_{rd} - \omega_r \sigma L_r i_{rq} + \dfrac{M}{L_s} \dfrac{d\phi_s}{dt} \\ v_{rq} = (R_r + p\sigma L_r) i_{rq} + \omega_r \sigma L_r i_{rd} + \omega_r \dfrac{M}{L_s} \phi_s \end{cases} \quad (7)$$

with: $\sigma = 1 - \dfrac{M^2}{L_s L_r}$ is leakage factor.

In addition, while resistance of the stator R_s is neglected (that is legitimate for medium and large machines) and ϕ_s is supposed constant (steady grid), thus:

$$\frac{d\phi_s}{dt} = 0 \ ; \ v_{sd} = 0 \ ; \ v_{sq} = v_s = \omega_s \phi_s \quad (8)$$

Then $P_s = -\dfrac{M}{L_s} v_s i_{rq}$ and $Q_s = -\dfrac{M}{L_s} v_s i_{rd} + \dfrac{V_s^2}{L_s \omega_s}$ (9)

It can be noticed that active power and reactive powers are independently controlled respectively by quadrature and direct rotor currents.

The Fig. 4 shows the internal functional diagram of the DFIG in PQ control purpose.

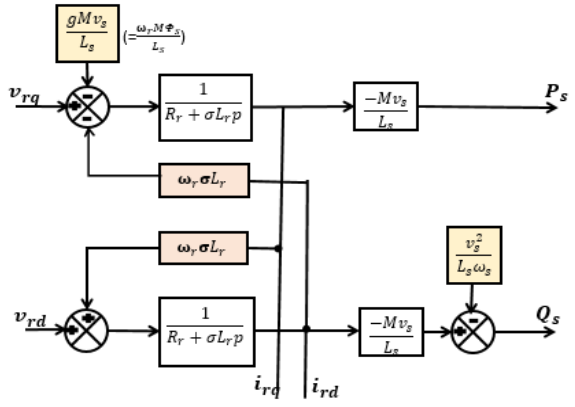

Fig. 4. Internal functional diagram of DFIG for PQ control purpose

Currents and voltages are linked by same first order transfer function $H(p) = \dfrac{1}{R_r + \sigma L_r p}$ with a cross coupling that should be compensated as shown in Fig. 5.

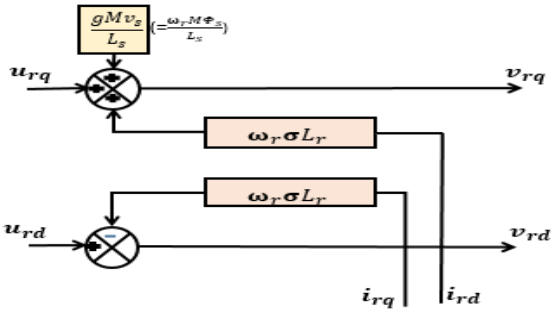

Fig.5. Decoupling bloc

The rotor currents i_{rd} and i_{rq} are now linked to compensated rotor voltage u_{rd} and u_{rq} as follow:

$$\begin{cases} u_{rd} = R_r i_{rd} + \sigma L_r \dfrac{di_{rd}}{dt} \\ u_{rq} = R_r i_{rq} + \sigma L_r \dfrac{di_{rq}}{dt} \end{cases} \quad (10)$$

IV. SLIDING MODE CONTROL OF ACTIVE AND REACTIVE POWERS

Sliding Mode Control (SMC) is nowadays frequently used because of its simplicity and insensitivity to parameters variations and externals disturbances [16].

The principle of this variable structure control consists in bringing a state vector of the system to a sliding surface and force it to stay. Once this surface reached, dynamics of the system are then imposed by this one, independently of disturbances and parameters variations of the model.

A. Conventional Sliding Mode Control (SMC)

Sliding surface for active power is defined by:

$$S(P) = P_s^{ref} - P_s \text{ and } \dot{S}(P) = \dot{P}_s^{ref} - \dot{P}_s \quad (11)$$

From (9) we deduct $\dot{S}(P) = \dot{P}_s^{ref} + v_s \dfrac{M}{L_s} \dfrac{di_{rq}}{dt}$ (12)

From (10), $\dfrac{di_{rq}}{dt} = \dfrac{1}{\sigma L_r}(u_{rq} - R_r i_{rq})$ (13)

hence, $\dot{S} = \left[\dot{P}_s^{ref} - \dfrac{R_r M v_s}{\sigma L_s L_r} i_{rq} \right] + \dfrac{M v_s}{\sigma L_s L_r} u_{rq}$ (14)

We put:

$$u_{rq} = u_{rq}^N + u_{rq}^D \quad (15)$$

(N for Nominal and D for discontinuous)

Then,

$$\dot{S} = \left[\dot{P}_s^{ref} + \frac{M v_s}{\sigma L_s L_r} u_{rq}^N - \frac{R_r M v_s}{\sigma L_s L_r} i_{rq} \right] + \frac{M v_s}{\sigma L_s L_r} u_{rq}^D \quad (16)$$

We choose:

ISSN 2356-5608

$$u_{rq}^{N} = -\frac{\sigma L_s L_r}{M v_s}\dot{P}_s^{ref} + R_r i_{rq} \quad (17)$$

to cancel the first term between brackets.

And then $\dot{S} = \frac{M v_s}{\sigma L_s L_r} u_{rq}^{D}$ (18)

Thus, $S\dot{S} = \frac{M v_s}{\sigma L_s L_r} u_{rq}^{D}.S$ (19)

By wisely choosing

$u_{rq}^{D} = -Ksign(S)$ with $K > 0$, (20)

Equation (19) becomes

$$S\dot{S} = -\frac{M v_s}{\sigma L_s L_r} KSsign(S) = -\frac{M v_s}{\sigma L_s L_r} K|S| \quad (21)$$

Stability condition of Lyapunov ($S\dot{S} < 0$) is then permanently assured.

Finally, the SMC law for Active Power is:

$$\begin{cases} S = P_s^{ref} - P_s \\ u_{rq} = u_{rq}^{N} + u_{rq}^{D} \\ u_{rq}^{N} = -\frac{\sigma L_s L_r}{M v_s}\dot{P}_s^{ref} + R_r i_{rq} \\ u_{rq}^{D} = -Ksign(S) \; with \; K > 0 \end{cases} \quad (22)$$

By the same approach, SMC reactive power law is:

$$\begin{cases} S = Q_s^{ref} - Q_s \\ u_{rd} = u_{rd}^{N} + u_{rd}^{D} \\ u_{rd}^{N} = -\frac{\sigma L_s L_r}{M v_s}\dot{Q}_s^{ref} + R_r i_{rd} \\ u_{rd}^{D} = -Ksign(S) \; with \; K > 0 \end{cases} \quad (23)$$

Synoptic scheme is shown in Fig. 6.

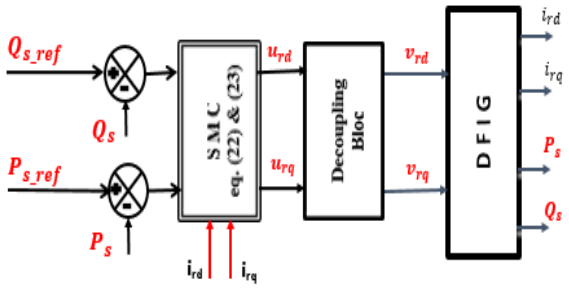

Fig. 6 . Synoptic Scheme for PQ Control.

Theoretically, any positive value of K can then assure the stability. Unfortunately, it is true only in ideal case where parameters are constant.

The minimum value of K assuring permanently the stability $S\dot{S} < 0$ even if parameters vary is defined by:

$$K_{\min} = 0.8 R_r \frac{P_s L_s}{M v_s} \quad (24)$$

Calculation for (24) is based on variation range estimation around nominal value for each parameter that will be detailed in future work.

According to our DFIG parameters given in appendix, we obtain $K_{\min} = 14$. And for our simulation results, we use $K = 15$ for P_s and $K = 30$ for Q_s .

B. Adaptive Sliding Mode Control (ASMC)

Contrary to the previous case where the gain K is fixed, we intend to establish a command law that allows to adjust the gain K until the sliding mode becomes established. The purpose is to increase the convergence speed when the gain is not sufficient, and save energy when the gain is oversized requesting pointlessly the system.

Adaptive command variable is:

$$u = -K(t)sign(S) \quad (25)$$

where $K(t)$ is the time varying gain.

The gain adaptation law relies on the observation of the N last states of the sliding variable (duration of $N\tau$ where τ is the sampling time) as shown in Fig.7.

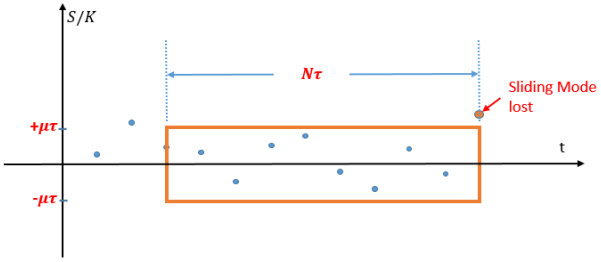

Fig. 7. Adaptive Sliding Mode Approach.

It is demonstrated in [17] that the precision for a first order sliding mode is proportional to τ .

We define the sliding surface as a rectangle with width proportional to τ ($[-\mu\tau, +\mu\tau]$) and length equal to $N\tau$ as depicted in Fig.7.

$K(t)$ variation is made exponentially or linearly depending on status of the system that is informed by $\alpha(t)$ [12, 18]:

$$\dot{K}(t) = \begin{cases} -\alpha(t)\lambda K(t) & if \quad K(t) > K_M \\ -\alpha(t)\lambda & if \quad K_m < K(t) < K_M \\ \lambda_m & if \quad K(t) < K_m \end{cases} \quad (26)$$

where

$$\alpha(t) = \begin{cases} +1 \; if \; \forall t_j \in [t - N\tau, t], \left|\frac{S(t_j)}{K(t_j)}\right| < \mu\tau \\ -1 \; if \; \exists t_j \in [t - N\tau, t], \left|\frac{S(t_j)}{K(t_j)}\right| > \mu\tau \end{cases} \quad (27)$$

and λ , μ , λ_m , K_m , and K_M are fixed according to dynamic requested and to ensure the stability [12, 18].

For our simulations results $\mu\tau = 200$, $K_m = 1$, $K_M = 5$, $\lambda = \lambda_m = 6$.

ISSN 2356-5608

C. Simulations and Comparison

Simulation is made by hardly submitting the system to reference profiles of active and reactive power as illustrated in Fig.8. In practice, variations of P_s^{ref} and Q_s^{ref} are not instantaneous but made according to defined ramps.

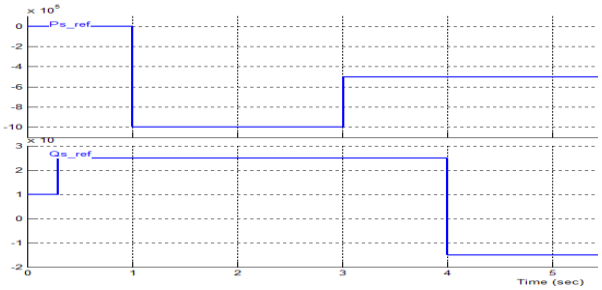

Fig. 8. Waveforms of P_s^{ref} and Q_s^{ref}

The simulation results are given in Fig.9 and Fig.10 for SMC and in Fig.11 and Fig.12 for ASMC.

It can be noted that exceeding rates are drastically improved with ASMC in comparison with conventional SMC. In fact, exceeding rates are reduced from 6% to 1% for Active Power and from 11.3% to 0.7% for Reactive Power. Moreover, ASMC presents less chattering and it is faster than SMC.

Furthermore, cross coupling effects, that may remain when using linear controllers such as PI, are here definitely disappeared with ASMC as well with SMC.

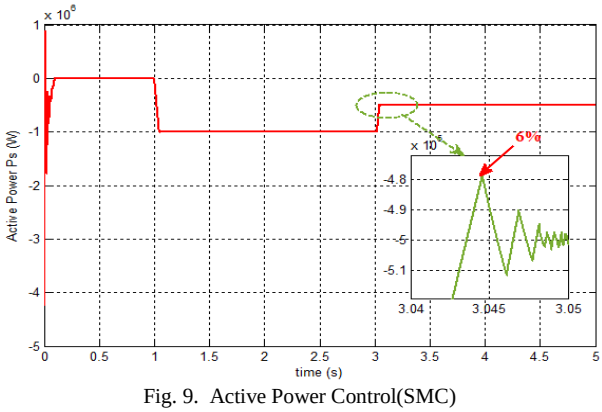

Fig. 9. Active Power Control(SMC)

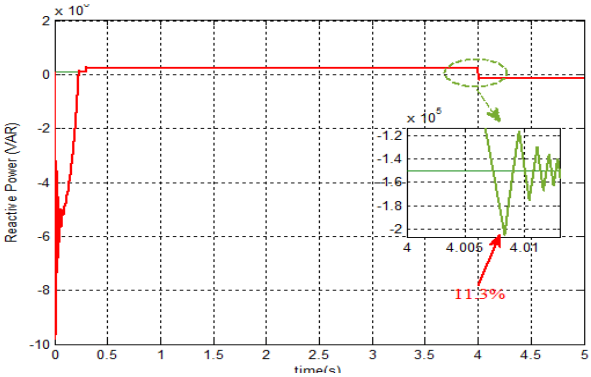

Fig. 10. Reactive Power Control (SMC)

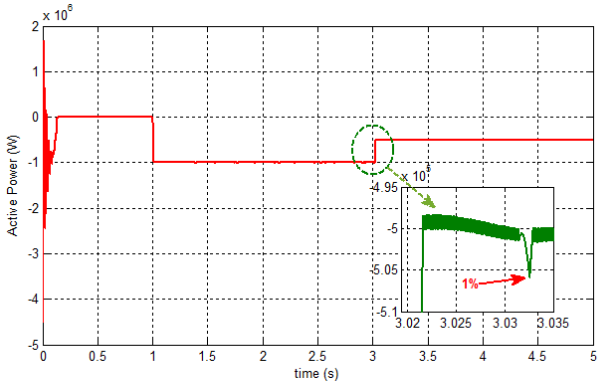

Fig. 11. Active Power Control (ASMC)

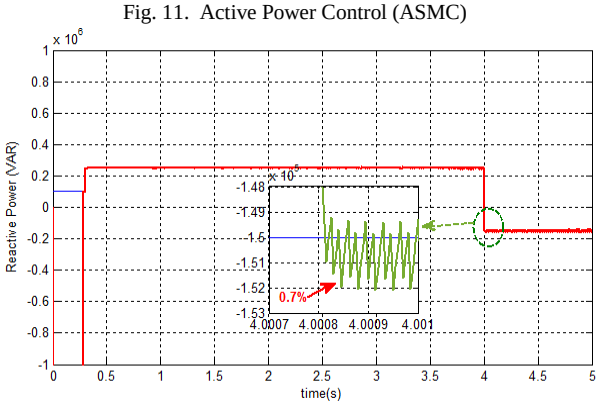

Fig. 12. Reactive Power Control (ASMC)

Robustness against parameters and external disturbances is confirmed for both controllers but it is better with ASMC.

Fig.13 shows the robustness of SMC against stator resistance R_s that it was increased by 50% and 100% from its rated value while Fig.14 shows its robustness to stator inductance L_s that was increased by 10% and 20% from its rated value.

Fig.15 and Fig.16 confirm the higher robustness of ASMC to the same parameters with same variations. It can be noticed that response time of ASMC and its chattering amplitude are reduced by more than 50% compared with SMC.

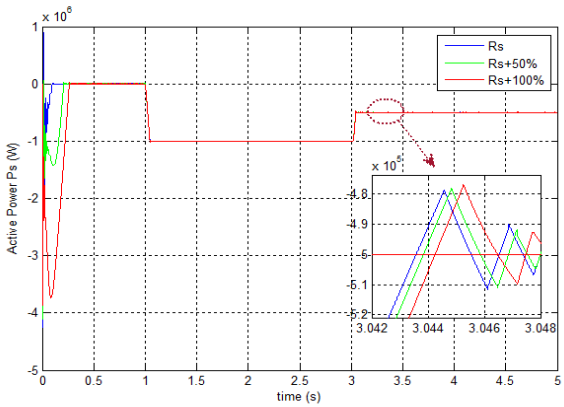

Fig. 13. Robustness of SMC to Stator Resistance Rs

ISSN 2356-5608

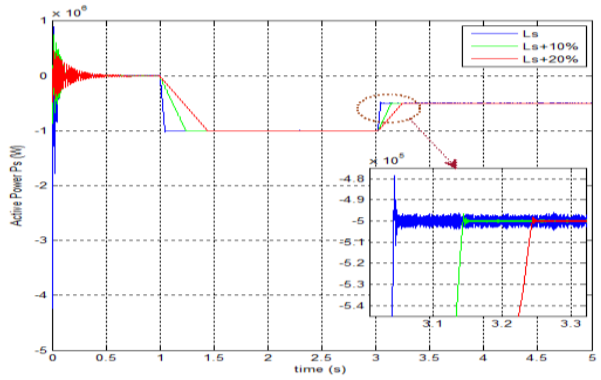

Fig. 14. Robustness of SMC to Stator Inductance Ls

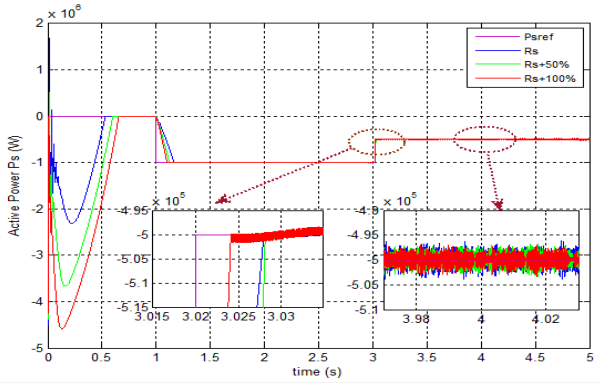

Fig. 15. Robustness of ASMC to Stator Resistance Rs

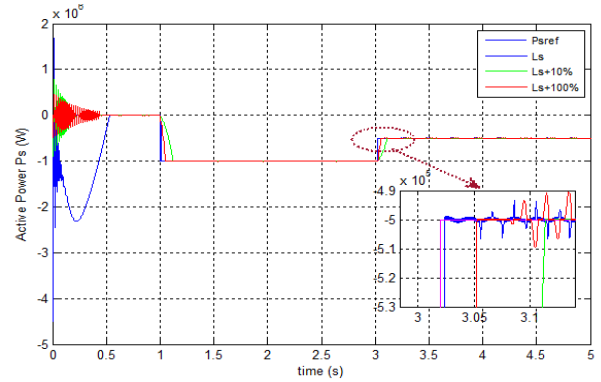

Fig. 16. Robustness of ASMC to Stator Inductance Ls

VI. CONCLUSION

The main contribution of this work is to show how to track any references of active and reactive powers with high dynamic performances using Sliding Mode Controllers. In addition of its response time improvement by at least 50% and its very important reduction of chattering compared with conventional Sliding Mode Controller, Adaptive Sliding Mode Controller has irreproachable robustness to parameters variations and external disturbances.

APPENDIX

DFIG parameters: $S_N = 3MVA$; $R_s = 0.012\Omega$; $R_r = 0.021\Omega$;

$L_s = 0.0137H$; $L_r = 0.0136H$; $M = 0.0135H$; $p = 2$;

$J = 0.07Kg.m^2$; $f = 0.0024N.m.s^{-1}$. Gear-Box: $G = 90$.

Turbine parameters: $P_{tN} = 4MW$; $R = 35.25m$

$c_1 = 0.5872, c_2 = 116, c_3 = 0.4, c_4 = 5, c_5 = 21, c_6 = 0.0085$

REFERENCES

[1] REN21, "RENEWABLES 2016 GLOBAL STATUS REPORT," Renewable Energy Policy Network for 21st Century, 2016.

[2] T. G. W. E. Outlook, "GWEO," 2012.

[3] windpower, "Wind Energy Could Supply 12% Of Global Electricity By 2020," 2012.

[4] ALTERNATIVE ENERGY, "www.altenergy.org/renewables/wind," 2016. [Online].

[5] GWEC, "Global Wind 2015 Report," April-2016.

[6] A. CHAIBA, Commandes intelligentes de la génératrice asynchrone double alimentée, PAF (Presse Académique Francophones), 2012, pp. 32-35.

[7] R. Babouri, D. Aouzellag and K. Ghedamsi, "Integration of Doubly Fed Induction Generator Entirely Interfaced With Network in a Wind Energy Conversion System," *ScienceDirect, Energy Procedia 36 (2013).*

[8] S. Abdeddaim and A. Betka, "Optimal Tracking and robust control of the DFIG wind turbine," *Electrical Power and Energy Systems, ELSEVIER*, vol. 49, 2013.

[9] Mohamed BENKAHLA, Rachid TALEB and Zinelaabidine BOUDJEMA, "Comparative Study of Robust Control Strategies for a DFIG-Based Wind Turbine," *IJACSA, vol.7, No.2*, 2016.

[10] F. Arama, B. Mazari, A. Dahbi, K. Roummani and M. Hamouda, "Artificial Intelligence control applied in wind energy system," *IEEE*, 2014.

[11] M. Hagh, S. Roozbehani, F. Najaty, S. Ghaemi, Y. Tan and K. Muttaqi, "Direct Power Control of DFIG based Wind Turbine based on Wind Speed Estimation and Particle Swarm Optimization," *IEEE*, 2015.

[12] M. Taleb, A. Levant and F. Plestan, "Pneumatic actuator control: solution based on adaptative twisting and experimentation," *Control Engineering Practice, 48 (5)*, 2013.

[13] A. Chemidi, Sidi Mohammed Meliani and Mohammed Choukri Benhabib, "Etude d'une Ferme éolienne à base de MADA connectée au réseau électrique: Analyse et compensation des harmoniques," in *CIGE-2013*, Bechar University, 2013.

[14] "GRID CODE FOR RENEWABLE ENERGIES," *WORKSHOP - EMI- Rabat*, June 2nd, 2015.

[15] J.-P. CARON and J.-P. HAUTIER, Modélisation et Commande de la Machine Asynchrone, TECHNIP, 1995.

[16] N. Khemiri, Adel Khelder and M.F. Mimouni, "Wind Energy Conversion System using DFIG Controlled by Backstepping and Sliding Mode Strategies," *IJRER, Vol.2, No.3*, 2012.

[17] A. LEVANT, "Homogeneity approach to high-order sliding mode design," *Automatica, Vol.41*, 2005.

[18] G. Bartolini, A. Levant, F. Plestan and M. Taleb, "Adaptation sliding mode," *IMA Journal of mathematical control and information*, 2013.

ISSN 2356-5608